

Modelling of an annular photocatalytic reactor

M. Marečić · F. Jović · V. Kosar · V. Tomašić

Received: 7 January 2011/Accepted: 25 February 2011/Published online: 9 March 2011
© Akadémiai Kiadó, Budapest, Hungary 2011

Abstract This work deals with the photocatalytic oxidation of toluene at room temperature and atmospheric pressure in the gas phase. The differential equations of the reactor model are solved numerically with simultaneous estimation of the model parameters. Estimation of the kinetic data is performed using a modified differential method of data analysis and a Nelder–Mead method of nonlinear optimization for parameter estimation. The reaction is performed in an annular photoreactor using UVA black light blue fluorescent lamp. The experiments are carried out at different total flow rates of the reaction feed ($20\text{--}160 \text{ cm}^3 \text{ min}^{-1}$), two different inlet concentrations of toluene (2.67 and 5.24 g m^{-3}) and at constant relative humidity (25%). A good agreement between the experimental data and theoretical predictions is obtained, supporting the applicability of the proposed models to describe the investigated process performed in laboratory annular photoreactor.

Keywords Annular reactor · Mathematical models · Photocatalytic oxidation · Toluene

List of symbols

a	Geometric surface area (m^2)
A_R	Surface area of reactor (annulus) cross-section (m^2)
C_A	Toluene concentration (g m^{-3})
$C_{A,0}$	Inlet toluene concentration (g m^{-3})
$C_{A,g}$	Toluene concentration in the fluid phase (g m^{-3})
$C_{A,s}$	Toluene concentration at the solid phase (g m^{-3})

M. Marečić

Department of Food Technology and Biotechnology, University of Zagreb, Zagreb, Croatia

F. Jović · V. Kosar · V. Tomašić (✉)

Department of Chemical Engineering and Technology, University of Zagreb, Zagreb, Croatia

e-mail: vtomas@fkit.hr

$\overline{C}_{A,t}$	Average toluene concentration in the fluid phase (g m^{-3})
D_A	Molecular diffusion coefficient of toluene in air ($\text{m}^2 \text{s}^{-1}$)
k_A	Reaction rate constant (min^{-1})
k_g	Interphase mass transfer coefficient (m h^{-1})
N	Number of the experimental points (dimensionless)
r	Radial reactor coordinate (m)
r_A	Reaction rate ($\text{mol h}^{-1} \text{kg}^{-1}$)
R	Diameter of reactor annulus (m)
SD	Root of the mean square deviation (dimensionless)
u	Superficial fluid velocity (m h^{-1})
u_m	Mean superficial fluid velocity (m h^{-1})
v_0	Volume flow rate ($\text{m}^3 \text{h}^{-1}$)
V	Reactor volume (m^3)
X_A	Toluene conversion (dimensionless)
z	Axial reactor coordinate (m)
Z	Length of the reactor (m)

Greek letters

κ	Ratio of inner and outer reactor diameter (dimensionless)
τ	Space time (min)

Dimensionless parameters

Re	Reynolds number (dimensionless)
Sc	Schmidt number (dimensionless)
Sh	Sherwood number (dimensionless)

Introduction

Photocatalytic oxidation using semiconductors as photocatalysts represents an excellent technology for environmental remediation. In particular, photocatalytic oxidation based on TiO_2 has been demonstrated to be highly effective in the treatment of contaminated water and air [1–11]. Photooxidation on TiO_2 surface irradiated with suitable UV radiation leads to the degradation and complete mineralization of volatile organic compounds (VOCs) into environmentally friendly species without significant energy input. The process is simple and requires only standard room conditions and stable and nontoxic catalyst. Degussa TiO_2 catalyst (P-25) has been, and continues to be the preferred choice in many studies in this field due to its high activity. Other photocatalyst include ZnO , ZnS , CdS , etc., but these are less active [1].

Although many studies have investigated the photocatalytic oxidation of gas-phase volatile organic compounds by using TiO_2 , most of them focused on reaction rate and reactor performance, as well as on the identification of reaction by-products [12–16]. Different photoreactor configurations are reported in the references [8, 17–22]. Generally, the photocatalytic reactors in use for air treatment can be categorized

according to: (a) gas flow geometry (tubular, annular, flat plate), (b) type of their light sources or (c) the way by which the photocatalyst is introduced into the system [23]. However, there is still a lack of mathematical models that can be applied to photocatalytic reactor design and scale-up. Different mathematical models are applied depending on photoreactor configuration, such as fixed bed annular reactor [24–28], batch reactor [18, 29–31], plane plate reactor [28, 32–34], honeycomb monolith reactor [17], microchannel reactor [35], annular Venturi reactor [18], etc.

The objective of the present research was to investigate the sensitivity of a gas-phase photocatalytic reaction to reaction conditions with respect to air pollutant such as toluene and to propose appropriate mathematical models. The proposed models can be used as a tool for designing and simulating the behavior of a photocatalytic annular reactor with titanium dioxide based materials as oxidation catalyst.

Experimental

Preparation and characterization of photocatalyst

The commercial TiO_2 powder catalyst supplied by Degussa (P25) was used to prepare the catalyst layer. The sodium silicate-modified TiO_2 was coated on the internal glass surface of the outer tube of an annular reactor and used for conducting the photoreactivity experiments. The interior tube of the annular reactor was made of quartz, due to its UV-conducting nature. Catalyst characterization was performed by several techniques, such as X-ray powder diffraction (XRD), Fourier transform infrared (FTIR) spectroscopy and surface measurements (adsorption/desorption of nitrogen at 77 K). A detailed description of catalyst preparation and characterization can be found elsewhere [25].

Reactor and experimental set-up

The reaction was performed at room temperature in an annular photocatalytic reactor designed to study the treatment of different organic pollutants in the gas phase. Toluene, as one of the typical organic compounds indoors, was used as a model VOC in this study. The reacting gaseous mixture consisted of toluene, air and water in various ratios. The reactant mixture was generated by bubbling air through saturators containing bidistilled water and toluene (LiChrosolv[®], Merck) at room temperature. High purity synthetic air was used as a carrier gas. Before switching on the UV-lamp, the gas mixture was fed into the reactor in order to achieve the equilibration of the catalyst with the reagents. The toluene concentration at the end of this period was taken as the initial value ($C_{A,0}$). Illumination of the catalyst was provided by an 8 W fluorescent black light blue lamp (Sylvania[®]). Space time in the reactor was varied by changing total flow rate of gas mixture at the constant reactor volume or reactor length. Conversion, X_A , was calculated with respect to toluene concentration.

Sampling and analysis

Samples of 0.5 ml were withdrawn periodically using a gas sampling valve, and the toluene concentration was measured on-line by a gas chromatograph (Varian 3300) equipped with Carbowax 20 M packed column (Restek) and FID detector. The reaction was performed under steady-state conditions. Toluene degradation was not detected in the dark or in the absence of catalyst. Thus, all variations in toluene concentration were ascribed to the photocatalytic activity of the catalyst. More details about the experimental apparatus and procedures are given elsewhere [25].

Results and discussion

Modelling of an annular photocatalytic reactor

Assumptions and governing equations

This study deals with specific aspects associated with mathematical modelling of the annular photocatalytic reactor. The approach to modelling an annular reactor is similar to modelling other similar reactor configurations. Generally, mathematical models can range from very simple to some very complex ones. The required degree of sophistication depends on the process and the reaction mechanism, and on its sensitivity to changing in the operating conditions. The degree of accuracy with which the kinetic and transport parameters are known is of equal importance. Avoiding unnecessary complexity is recognized as a general rule.

In this work, three different heterogeneous reactor models, accounting for a 1D (Model I) and 2D description of gas phase (Model II and III), were applied for modelling and simulating the annular photocatalytic reactor. Fig. 1 shows the scheme of the channel inside the annular reactor with the basic features of a 2D heterogeneous model (Model III). The main assumptions applied to all three models were: steady-state conditions, negligible pressure drop along the reactor, and the reaction was assumed to occur on the surface of the catalyst.

According to the 1D model, the mass transfer of reactant (toluene) from the main stream (bulk) to the catalyst surface is located in the thin boundary layer, in which only concentration gradient exists. This means that the whole transfer resistance is defined by the convective mass transfer coefficient, depending on gas properties and hydrodynamic conditions. It is natural to assume that the transfer of toluene molecules from the gas phase is due to diffusion across the whole diameter of free space between inner and outer tube. 2D models consider this fact and suppose the mass transfer to the catalyst layer by diffusion. The most important difference between proposed 2D models (Model II and Model III) is in the regime of fluid flow. Model II considers ideal flow conditions, and Model III takes laminar flow into consideration. More realistic, of course, is the assumption of the laminar flow, which can be confirmed by calculating the Reynolds number. For both 2D models, the molecular coefficient of toluene diffusion in the reaction mixture is required as a parameter in model equations. The value of this parameter can be calculated from

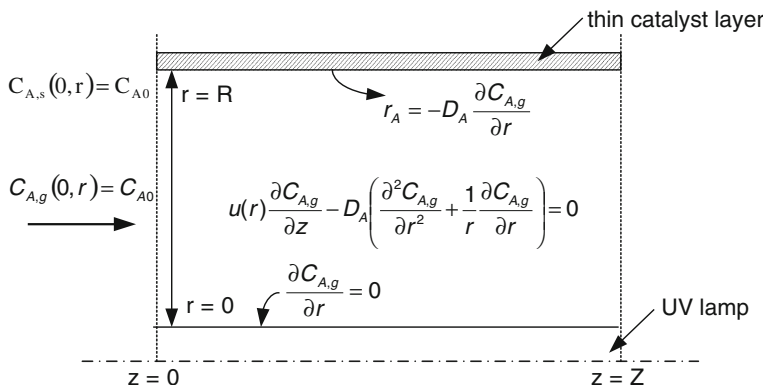


Fig. 1 Scheme of the channel inside the annular reactor including mass transfer effects according to assumptions of the 2D model (Model III)

the data in the references. Reaction rate constants and mass transfer coefficients are the estimated parameters in 1D model. The mass transfer coefficient can be calculated from empirical correlations, and the obtained value is a measure of goodness of fit with experimental results. In the 2D models, the only fitting parameter is the reaction rate constant, because the molecular diffusion coefficient is taken as a known value. The other assumptions used to develop the models were steady-state and isothermal conditions. A gas mixture flows through the reactor under constant volume velocity and concentration of all present substances. Ideal flow was proposed for Model I and II, and laminar flow was proposed for Model III. Axial diffusion in the gas phase was neglected. The catalyst was deposited on the inner wall of the outer tube in a very thin layer and intraphase diffusion in the reaction path was negligible. Deactivation of the catalyst was neglected because of the rapidly achieved stationary conversion of toluene and frequently changing catalyst layer. Model equations are summarized in Table 1. The simple pseudo first-order kinetic model was used to describe the kinetics of toluene photooxidation.

Numerical approach for the model solution

The derived heterogeneous models are given by mass balances of toluene, as shown in Table 2. Computer algorithms were developed in the program package *Matlab*[®]. Model I was solved by Runge–Kutta method for ordinary differential equations (ODE). Models II and III, represented with partial differential equations (PDE), were solved using the method of lines [36]. By using this method, model equations were discretized along the axial and radial coordinates by backward differences. The inlet conditions for the Models II and III were the same as for Model I (Eq. 3). The mass transfer coefficient (k_g) was calculated using Eq. 5, taking into account the correlation with the corresponding Sh number, while the value of the molecular diffusion coefficient of toluene in air, D_A , was taken from the literature ($0.0804 \text{ cm}^2 \text{ s}^{-1}$) [37]. All computations were performed only with one estimated

Table 1 Model equations used in this study*Model I-1D heterogeneous model*

$$r_A = f(C_{A,S}) = k_g a (C_{A,g} - C_{A,S}) \quad (1)$$

$$u \frac{dC_A}{dz} = k_g a (C_{A,g} - C_{A,S}) \quad (2)$$

The inlet conditions:

$$C_{A,S} = C_{A,g} = C_{A_0}, \text{ at } z = 0 \quad (3)$$

The kinetic model:

$$r_A = k_A C_A \quad (4)$$

Interphase mass transfer coefficient, k_g :

$$k_g = \frac{Sh D_A}{2R(1-k)} Sh = 0.705 \left(Re \frac{1}{2(1-k)} \right)^{0.43} Sc^{0.6} \quad (5)$$

Model II-2D heterogeneous model (ideal flow conditions)

$$u \frac{\partial C_{A,g}}{\partial z} - D_A \left(\frac{\partial^2 C_{A,g}}{\partial r^2} + \frac{1}{r} \frac{\partial C_{A,g}}{\partial r} \right) = 0 \quad (6)$$

$$r_A = -D_A \frac{\partial C_{A,S}}{\partial r} \Big|_{r=R} \quad (7)$$

The inlet conditions: the same as defined by Eq. 3

The kinetic model: the same as defined by Eq. 4

The boundary conditions:

$$\text{Boundary condition at the wall of inner tube: } \frac{\partial C_{A,g}}{\partial r} = 0, \text{ at } r = 0 \quad (8)$$

$$\text{Boundary condition at catalyst surface: } D_A \frac{\partial C_{A,S}}{\partial r} = -k_A C_{A,S}, \text{ at } r = R \quad (9)$$

Model III-2D heterogeneous model (laminar flow conditions)

$$u(r) \frac{\partial C_{A,g}}{\partial z} - D_A \left(\frac{\partial^2 C_{A,g}}{\partial r^2} + \frac{1}{r} \frac{\partial C_{A,g}}{\partial r} \right) = 0 \quad (10)$$

$$r_A = -D_A \frac{\partial C_{A,S}}{\partial r} \Big|_{r=R} \quad (11)$$

$$u(r) = 2u_m \left[1 - \left(\frac{r}{R} \right)^2 \right], \quad u_m = \frac{v_0}{A_R} \quad (12)$$

The inlet conditions: the same as defined by Eq. 3

The kinetic model: the same as defined by Eq. 4

The boundary conditions:

$$\text{Boundary condition at the wall of inner tube: } \frac{\partial C_{A,g}}{\partial r} = 0, \text{ at } r = 0 \quad (13)$$

$$\text{Boundary condition at catalyst surface: } D_A \frac{\partial C_{A,S}}{\partial r} = -k_A C_{A,S}, \text{ at } r = R \quad (14)$$

Table 2 Comparison of results obtained by 1D and 2D heterogeneous models

$C_{A,S}$ g m ⁻³	Model I		Model II		Model III	
	k_A/min^{-1}	SD	k_A/min^{-1}	SD	k_A/min^{-1}	SD
2.67	1.0582	0.0127	1.0184	0.0118	1.0426	0.0116
5.24	0.4515	0.0212	0.4534	0.0212	0.4550	0.0213
$\overline{SD} = 0.0170$		$\overline{SD} = 0.0165$		$\overline{SD} = 0.0164$		

parameter, e.g. reaction rate constant, k_A , in order to avoid uncertainty due to a great number of parameters. Parameter estimation was performed using a modified differential method of data analysis and the Nelder–Mead method of non-linear

optimization. The correlation criterion was the root mean square deviation between the experimentally obtained and theoretically predicted values, SD:

$$SD = \frac{1}{N} \sqrt{\sum_1^N (C_{A,e} - \bar{C}_{A,t})^2} \quad (15)$$

Average (i.e. “mixing cup”) toluene concentration in the fluid phase was calculated using Eq. 16,

$$\bar{C}_{A,t} = \frac{1}{v_0} \int_0^R C_{A,t}(r) u(r) 2\pi r dr \quad (16)$$

Model results and analysis

The photocatalytic oxidation of toluene in an annular reactor is an example of a complex reaction system. Therefore, it is a challenge to develop the appropriate mathematical model in order to describe this reaction system. Computer simulation of an annular photocatalytic reactor needs a basic choice between one-dimensional and two-dimensional model. A pragmatic choice should be based on the compared evaluation of the reliability and the complexity of mathematical models. It is well known that the 2D model with the proper boundary conditions can describe real transport phenomena inside the annular reactor, while the one-dimensional model requires a prior estimation of the mass transfer coefficient.

Fig. 2 shows a set of typical oxidation results predicted by the heterogeneous 1D model obtained at inlet toluene concentration of 2.67 and 5.24 g m⁻³, respectively. As expected, the conversion of toluene increases by increasing space time in the reactor, and obviously, at the end, leads to final equilibrium conversion. Conversion of toluene decreases with increased inlet toluene concentration in the whole range of the total flow rate. A similar dependence of the degradation rate on inlet contaminant concentrations is reported in the literature references [38]. These results can be attributed to a limited number of active sites on TiO₂ surface available for toluene adsorption. A satisfactory degree of correlation between the experimental values and values predicted by 1D heterogeneous model was established.

Similar results are obtained using more complex 2D heterogeneous models. The estimated values of the rate constant (k_A) and the root mean square deviation obtained using 1D and 2D models are given in Table 2. As it can be seen, the lower values of the root mean square deviation are obtained using 2D models, indicating that 2D models can probably be used with higher accuracy in order to describe the behavior of the annular reactor. Obviously, a more realistic picture of the annular reactor performance can be obtained using more complex 2D heterogeneous models, especially taking into consideration concentration gradients in the fluid phase (the place between interior and outer tube of the reactor) due to mass transfer by diffusion. In this case, the imaginary boundary layer (film), which is usually close to the interior wall of the outer reactor tube, is broadened over the whole space between the reactor’s two concentric tubes.

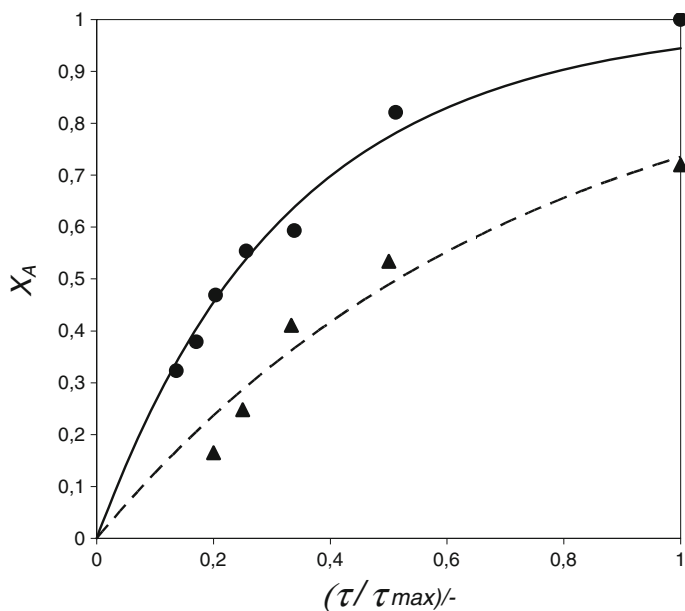


Fig. 2 Influence of the space time and the inlet toluene concentration on toluene conversion: experimental data (points), the values predicted by 1D heterogeneous model (lines). Reaction conditions: inlet toluene concentration: (filled circle) 2.67 g m^{-3} ; (filled triangle) 5.24 g m^{-3}

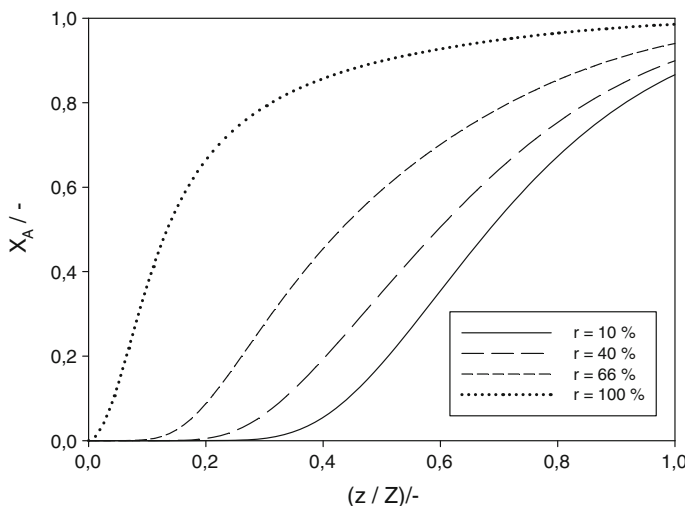


Fig. 3 Axial profiles of the toluene conversion in the gas phase of the annular reactor for different fractions of the overall reactor radius, where curve at 100% represents the values of conversion at the surface of TiO_2 layer along the reactor length (Model III). Reaction conditions: inlet toluene concentration: 5.24 g m^{-3}

The advantage of the 2D in comparison to the 1D heterogeneous model is its ability to predict conversion profiles along the reactor length (Fig. 3), as well as across the radius of the annular reactor (Fig. 4). According to the shape of these profiles, it is possible to draw some conclusions about the relationship between the rate of the interphase mass transfer and the reaction rate at the surface of TiO_2 layer.

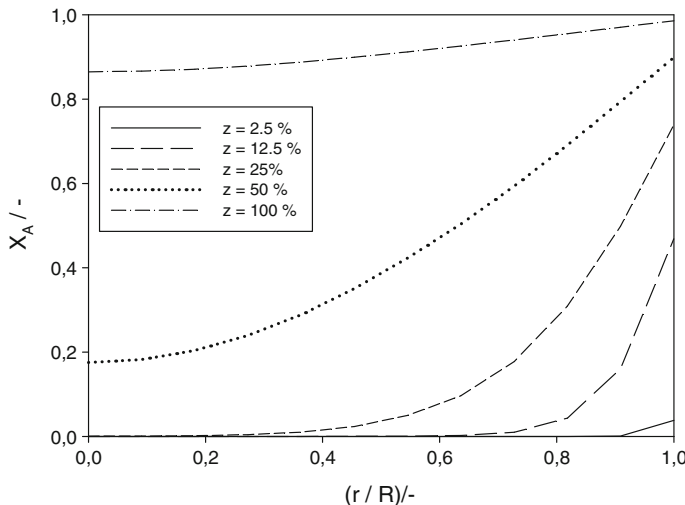


Fig. 4 Radial profiles of the toluene conversion in the gas phase of the annular reactor for different fractions of the overall reactor length, where the curve at 100% represents the values of conversion at the exit of reactor (Model III). Reaction conditions: inlet toluene concentration: 5.24 g m^{-3}

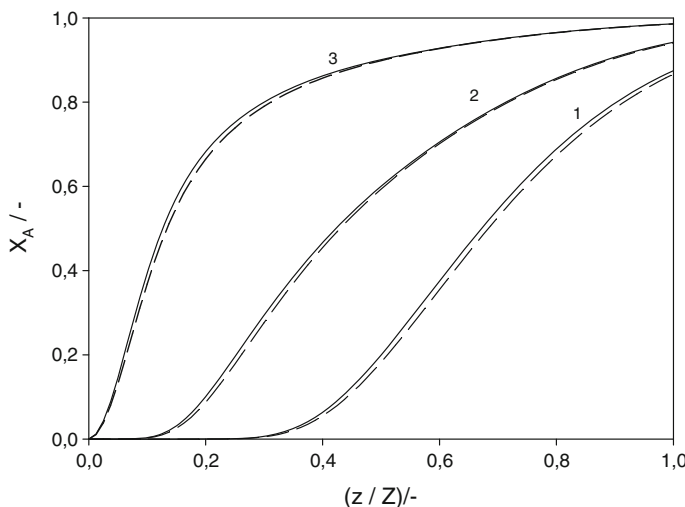


Fig. 5 Comparison of the axial profiles of toluene conversion predicted by the Model II (dashed line) and Model III (solid line) at different radial positions inside the reactor: 1- at $r = 10\%$, 2- at $r = 66\%$, 3- at $r = 100\%$

Apparently, the reaction rate is faster in comparison with the interphase diffusion. This can be supported by the high increase of toluene conversion near the surface of the catalyst layer ($r = 100\%$), especially at the entry of the reactor (see Fig. 3). However, along the reactor length, the conversion increases slower due to the fact that mean concentration in the fluid phase decreases along the reactor length not only due to the chemical reaction at the catalyst surface, but also due to the developing radial diffusion profile in the fluid phase. Fig. 5 shows the comparison of results obtained using Model II and Model III. As it can be seen from Fig. 5, almost the same results are obtained using both 2D models. Although the 2D models are rather complex, the benefit of their use is a better and more reliable prediction of reactor performance under a wide range of operating conditions.

Conclusions

This paper reports the results of experimental and theoretical investigation of the photocatalytic oxidation of toluene in the gas phase. Different mathematical models, such as 1D and 2D heterogeneous models based on ideal flow and laminar flow conditions, were used to simulate the behavior of a photocatalytic annular reactor with titanium dioxide as the oxidation catalyst. The proposed models were based on the physical picture, especially regarding the hydrodynamics of the gas phase inside the reactor and the mode of toluene transfer from gas phase to the catalytic surface. The 2D heterogeneous models were developed in order to predict the axial profile of conversion along the reactor length and the radial profile across the reactor radius. Differential equations of the reactor model were solved numerically with simultaneous estimation of the model parameter. All computations were performed only with one estimated parameter, e.g. reaction rate constant, k_A , in order to avoid uncertainty due to a great number of parameters. The proposed models were verified by comparing computer simulation data with the experimental laboratory results. Taking into account the root mean square deviation as a correlation criterion, better estimation results are obtained with 2D heterogeneous models. Generally, a good agreement between the experimental data and theoretical predictions was obtained, supporting the applicability of the proposed models to describe investigated process performed in the annular photocatalytic reactor.

Acknowledgments The authors highly appreciate the financial support that the Ministry of Science, Education and Sport of Republic of Croatia has given for this study.

References

1. De Lasa H, Serrano B, Salaices M (2005) Photocatalytic reaction engineering. Springer, New York
2. Michael STM, Hoffmann R, Choi W, Banemann DW (1995) Chem Rev 95:69
3. Zhao J, Yang X (2003) Build Environ 38:645
4. Bhatkhande DS, Pangarkar VG, Beenackers AACM (2001) J Chem Technol Biotechnol 77:102
5. Ollis DF (2000) CR Acad Sci Paris, Série Iic. Chimie/Chem 3:405
6. Fox MA, Dulay MT (1993) Chem Rev 93:341
7. Mills A, Lee SK (1992) J Photochem Photobiolog A Chem 152:233

8. Paz Y (2010) *Appl Cat B Environ.* doi:[10.1016/j.apcatb.2010.05.011](https://doi.org/10.1016/j.apcatb.2010.05.011)
9. Cao L, Gao Z, Suib SL, Obee TN, Hay SO, Freihaut JD (2000) *J Catal* 196:253
10. Mo J, Zhang Y, Xuz Q, Zhu Y, Lamson JJ, Zhao R (2009) *Appl Catal B Environ* 89:570
11. d'Hennezel O, Pichat P, Ollis DF (1998) *J Photochem Photobiolog A Chem* 118:197
12. Jeong J, Sekiguchi K, Lee W, Sakamoto K (2005) *J Photochem Photobiolog A Chem* 169:279
13. Mendez-Roman R, Cardona-Martinez N (1998) *Catal Today* 40:353
14. Xie C, Xu Z, Yang Q, Li N, Zhao D, Wang D, Du Y (1994) *J Mol Catal A Chem* 217:193
15. Alberici RM, Jardim WF (1997) *Appl Catal B Environ* 14:55
16. Nicollella C, Rovatti M (1998) *Chem Eng J* 69:119
17. Romero-Vargas Castrillón S, Ibrahim H, De Lasas H (2006) *Chem Eng Sci* 61:3343
18. Ibhodon AO, Arabatzis IM, Falaras P, Tsouklaris D (2007) *Chem Eng J* 133:317
19. Imoberdorf GE, Cassano AE, Irazoqui HA, Alfano OM (2007) *Catal Today* 129:118
20. Imoberdorf GE, Cassano AE, Irazoqui HA, Alfano OM (2007) *Chem Eng Sci* 64:1138
21. Furman M, Corbel S, Wild G, Zahraa O (2010) *Chem Eng Proc Proc Intensification* 49:35
22. Paz Y (2009) *Adv Chem Eng* 36:289
23. Wu JF, Hung CH, Yuan CS (2005) *J Photochem Photobiol A Chem* 170:299
24. Obuchi E, Sakamoto T, Nakano K (1999) *Chem Eng Sci* 54:1525
25. Tomašić V, Jović F, Gomzi Z (2008) *Catal Today* 137:350
26. Taghipour F, Mohseni M (2005) *AIChE J* 51(11):3039
27. Imoberdorf GE, Irazoqui HA, Alfano OM, Cassano AE (2007) *Chem Eng Sci* 62:793
28. Palmisano G, Addamo M, Augugliaro V, Caronna T, Paola AD, Lopez EG, Loddio V, Marci G, Palmisano L, Schiavello M (2007) *Catal Today* 122:118
29. Kim SB, Hwang HT, Hong SC (2002) *Chemosphere* 48:437
30. Zalazar CS, Martin CA, Cassano AE (2005) *Chem Eng Sci* 60:4311
31. Demeestere K, Visscher AD, Dewulf J, Leeuwen MV, Langenhove HV (2004) *Appl Catal B Environ* 54:261
32. Obee TN, Hay SO (1997) *Environ Sci Technol* 31:2034
33. Mehrdad Keshmiri TT, Mohseni Madjid (2006) *J Hazard Mat B* 128:130
34. Yu H, Zhang K, Rossi C (2007) *J Photochem Photobiol A Chem* 188:65
35. Ge H, Chen G, Yuan Q, Li H (2005) *Cat Today* 110:171
36. Schiesser WE (1991) *The numerical methods of lines. Integration of partial differential equations.* Academic Press, San Diego
37. <http://www.epa.gov/athens/learn2model/part-two/onsite/estdiffusion.html>
38. Bouzaza A, Vallet C, Laplanche A (2006) *J Photochem Photobiol A Chem* 177:212